Monitoring the dominance of higher-order chromatic dispersion with spectral interferometry using the stationary phase point method

Tímea Grósz [a,*], Attila P. Kovács [a], Katalin Mecseki [a,b], Lénárd Gulyás [a], Róbert Szipőcs [c]

[a] Department of Optics and Quantum Electronics, University of Szeged, Dóm tér 9, H-6720 Szeged, Hungary
[b] Blackett Laboratory, Imperial College London, Prince Consort Road, SW7 2BW London, United Kingdom
[c] Institute for Solid State Physics and Optics, Wigner RCP, Konkoly Thege út 29-33, H-1121 Budapest, Hungary

ABSTRACT

Simulations were performed in order to investigate whether the stationary phase point method can be used to estimate the dominance of higher-order dispersion of the optical element under study. It was shown that different higher-order dispersion terms may result in the appearance of more than one stationary phase point on the interferogram in contrast to common glasses having group-delay dispersion as the highest decisive term in their spectral phase. The results obtained by simulations were demonstrated experimentally with spectral interferometric measurements conducted on a photonic bandgap fiber sample and a prism pair. We concluded that from the shape, movement and number of the stationary phase points it is generally possible to predict which dispersion terms are the most significant, however, in some cases the retrieval of the coefficients is also necessary in order to rule out any ambiguity. The method can offer a dispersion monitoring possibility which is useful in quality testing of specialty fibers and when adjusting stretcher-compressor systems, for example.

© Elsevier B.V. All rights reserved.

1. Introduction

Nowadays there are countless applications relying on optical fibers which require precise control of certain characteristics, such as dispersion, birefringence or nonlinear behavior. Bragg-type [1] and photonic crystal fibers [2–5] have received considerable attention owing to their unique attributes, which can be tailored by the proper design of their geometrical structure. To date, a considerable amount of effort has been devoted to decrease the second-order, so-called group-delay dispersion (GDD) and the third-order dispersion (TOD) of the fibers, which are responsible for pulse broadening and post- or pre-pulses, respectively. Doing so, the fourth- (FOD) and higher-order dispersion become significant unlike in common materials which do not exhibit such dispersion characteristics.

A similar effect is observable in high power laser systems relying on chirped pulse amplification (CPA) [6]. Numerous solutions have been proposed to eliminate the GDD and the higher-order dispersion terms of the stretcher and the amplifier stage with the compressor in order to obtain nearly transform-limited pulses at the output of a CPA laser [7–14]. Nonetheless, reducing the GDD and the TOD generates uncompensated FOD in the system [13,14]

which might be of concern in applications requiring pulses with ultrahigh contrast. All in all, it can be concluded that reduction of the lower-order dispersion results in pronounced contribution of the higher-order dispersion which limits the performance of the fiber in pulse propagation or the achievable peak power in a CPA laser.

Retrieval of the pulse duration is of great prominence, however, when optimizing laser systems retrieval of the spectral phase is even more important as it shows the residual dispersion of the pulse. As certain pulse distortions can be associated with given dispersion terms, monitoring and precise measurement of the higher-order dispersion is essential. Numerous pulse diagnostic schemes have been invented, which can be divided into self-referencing and non-referencing schemes. The oldest self-referencing method the interferometric autocorrelation (IAC) accompanied by the pulse spectrum can be used to retrieve the pulse shape and the spectral phase, as various chirps produce distinctive patterns. Despite its benefits, the method contains an ambiguity in the sign of the chirp and moreover the accuracy of the chirp measurement is not very high [15]. Frequency-resolved optical gating (FROG) is another autocorrelation-type measurement possibility which has several implementations, such as polarization gate (PG), self-diffraction (SD), transient grating (TG), second- (SHG) or third-harmonic generation (THG) FROG [16]. PG FROG is a complete and unambiguous pulse characterization technique although requires high-quality polarizers thus it is very expensive.

* Corresponding author. Fax: +36 62 54 46 58.
E-mail address: tgrosz@titan.physx.u-szeged.hu (T. Grósz).

SD FROG, a bit cheaper solution which involves third-order non-linearity as well, is more sensitive to even-order temporal-phase distortions, but less to the odd-orders. TG FROG requires no polarizers and is more sensitive compared to the previous ones; however its need for three beams can be disadvantageous. SHG FROG involves only second-order nonlinearity, thus has a stronger signal. It is slightly less sensitive than IAC and has an ambiguity in the direction of time as well. THG FROG on the other hand removes the direction of time ambiguity but in turn is less sensitive than the SHG version. The method is more sensitive than the other previously mentioned third-order FROG methods, but it contains relative phase ambiguities unlike them. Another problem arises in the case of perfectly linearly chirped Gaussian pulses as the sign of the chirp parameter cannot be determined with THG FROG. Yet another technique, based on the modification of IAC, modified spectrum auto-interferometric correlation (MOSAIC) was developed for real-time dispersion control [17–20]. MOSAIC is very sensitive to chirp, even for lower values, as opposed to IAC, and produces distinctive patterns for different orders. It offers detection of the presence of chirp thus a real-time optimization possibility. Unfortunately, the same signal can be generated by several combinations of various order chirps and in addition to time direction ambiguity; accordingly, the method can be used only for qualitative determination. However, if not only the peak amplitude of the envelope of the interference minima of the MOSAIC signals are used, but also the temporal shape is studied quantitative information regarding the chirp can be required. The exact values of given terms can be obtained by iterative processes [18]. Different approaches were developed to reduce calculation time and remove uncertainties, such as envelope (E)-MOSAIC algorithm which, combined with measurement of differential fringe phase (DFP) using software control (LabVIEW) control yields a sign-sensitive phase retrieval technique [20]. Considering that in most cases a direct feedback is necessary, avoiding complicated, time-consuming data collecting methods would be favorable. Interferometric methods in general require the collection of less data than spectrographic methods, and thanks to their direct inversion algorithms they enable rapid pulse reconstruction. Spectral phase interferometry for direct electric field reconstruction (SPIDER) for instance is a promising candidate. Using LabVIEW adds to the relative easy implementation of the method [21]. A detailed comparison of IAC, two types of SPIDER and interferometric (I) FROG conducted by Stibenz et al. [22] revealed some considerations. It was concluded that IAC is of great service to verify other techniques, SPIDER becomes less reliable with increasing complexity of the pulses to be measured, a spatially encoded arrangement (SEA) of SPIDER gathers a large number of data thus it is less suitable for high data acquisition rates, but advantageous for complex, low energy pulses, and IFROG uses iterations to reconstruct the pulse and the phase, which need further improvements. In terms of simplicity cost one might consider using linear methods which do not require expensive high quality nonlinear crystals or 2D detection schemes. Spectral interferometry is a widely used extremely sensitive linear technique for dispersion characterization of different optical elements which does not necessarily require a laser and works fine with white light as well. For spectral phase retrieval there are more evaluation methods at our disposal. The precision of the Fourier-transform evaluation method in measuring higher-order dispersion is already demonstrated [23,24], however if dispersion retrieval in a wide wavelength range is of interest, thus a lower resolution spectrometer is used, the method becomes inaccurate. On the other hand, the so-called stationary phase point (SPP) method [25–29], also known as equalization wavelength, is one of the most common evaluation methods, the applicability of which has already been demonstrated in measuring the dispersion of various optical elements, including fibers

[23,24,30–32]. The SPP method is advantageous as regardless of the value of the dispersion and the resolution of the spectrometer the positions of the SPPs can be precisely determined [28]. Up until now this method was mainly used only in the case of optical elements and fibers where the GDD was the decisive dispersion term, however, recent studies show that even fifth-order dispersion (QOD) has significance when the GDD is reduced and the TOD becomes dominant [23,24]. In that case two SPPs were detected at certain delays, and the group delay curve was determined from the positions of both SPPs. Accordingly, it is worth investigating the possibility of forming more than two SPPs and whether their number suggest which is the highest decisive term in the spectral phase of the optical element or system under study. Moreover, a two-dimensional dispersion monitoring possibility in a pulse stretcher-compressor system has already been proposed employing the SPP method proving its adequacy for such purposes, however, only up to third-order dispersion [33]. It would be beneficial to investigate whether a cheaper implementation relying on a low resolution spectrometer using the SPP method can be used for the same purpose.

In this work we present a detailed study regarding the relation between the SPPs and the higher-order dispersion terms. We investigate the possibility of monitoring the dominance of the dispersion orders by studying the shape, movement and number of SPPs appearing on spectral interferograms. The effects of given dispersion terms up to the fifth order on the spectral interferogram are demonstrated using simulations. Measurements were performed on a Bragg-type solid-core photonic bandgap (PBG) fiber sample and a prism pair to demonstrate the usefulness of the method.

2. Theory

Spectral interferometry is a common tool in dispersion measurement and spectral phase retrieval of various optical elements. The technique utilizes a two-beam interferometer, usually a Michelson or Mach–Zehnder type, illuminated with a broadband light source, for instance an ultrashort pulse laser or a tungsten halogen lamp. The optical element or system, the dispersion of which is tested, is placed in one arm of the interferometer, while the other arm provides a reference and has adjustable path length. As the two beams from the sample and the reference arms interfere, fringes can be observed at certain arm length differences. The fringes can be studied utilizing a spectrometer placed at the output of the interferometer. The frequency-dependent intensity distribution $I(\omega)$ of the interference pattern can be written as

$$I(\omega) = I_s(\omega) + I_r(\omega) + 2\sqrt{I_s(\omega)I_r(\omega)}\,\cos(\Phi(\omega)), \qquad (1)$$

where I_s and I_r denote the spectral intensities of the sample and the reference beams, respectively, and Φ is the spectral phase difference between the arms

$$\Phi(\omega) = \varphi(\omega) + \frac{\omega}{c}(l_s - l_r) = \varphi(\omega) + \omega\tau. \qquad (2)$$

In Eq. (2) $\varphi(\omega)$ stands for the spectral phase of the sample, l_s and l_r are the path lengths of the light beams in the sample and the reference arms in air, respectively. We presumed that the refractive index of the air equals to 1, c denotes the velocity of light in vacuum and τ is the time delay arising from the arm length difference.

As an ultrashort laser pulse travels through a dispersive optical element or system, its temporal intensity profile undergoes a change that is only determined by the spectral phase introduced by the elements, assuming that the variation in the amplitude of

the spectral components of the pulse is negligible. Generally, the coefficients of the Taylor-expansion of $\varphi(\omega)$ are used to characterize the spectral phase function

$$\varphi(\omega) \approx \sum_{i=0}^{n} \frac{\varphi_n}{n!}(\omega - \omega_0)^n, \tag{3}$$

where ω_0 is the carrier frequency of the pulse, and

$$\varphi_n = \frac{d^n\varphi(\omega)}{d\omega^n}\bigg|_{\omega=\omega_0} \tag{4}$$

correspond to the nth derivatives of the spectral phase with respect to the angular frequency calculated at the carrier frequency. The consecutive coefficients φ_n are called as the constant phase term, the group delay (GD), the GDD, the TOD, the FOD and QOD. Considering, that specific pulse distortions can be related to these coefficients being dominant, they are usually also determined along with the spectral phase curve measurement.

Once the interferogram is recorded, the spectral phase can be retrieved in several ways. When utilizing the SPP method, the following steps are performed. First of all, the interferogram is normalized

$$\cos(\varPhi(\omega)) = \frac{I(\omega) - I_s(\omega) - I_r(\omega)}{2\sqrt{I_s(\omega)I_r(\omega)}}. \tag{5}$$

This normalization is not necessary but advisable as it improves the visibility of the interferogram and the identification of the SPP by canceling out the errors caused by the frequency-dependent spectrum. By studying the conditions when the first derivative of $\cos(\varPhi(\omega))$ in Eq. (5) becomes zero

$$\frac{d\cos(\varPhi(\omega))}{d\omega} = -\sin(\varPhi(\omega))\frac{d\varPhi}{d\omega} = 0, \tag{6}$$

i.e. when the extreme values are formed, the concept of this evaluation method becomes quite straightforward. Considering the case when Eq. (6) is fulfilled by the condition

$$\frac{d\varPhi}{d\omega} = 0, \tag{7}$$

it can be seen that at given frequencies a stationary phase point is formed, around which the phase changes very slowly. As the length of the reference arm is adjusted, the position of the SPP in the interferogram changes because the condition of forming an SPP is then fulfilled at a different frequency. By substituting Eq. (2) into Eq. (7) we get

$$\frac{d\varphi}{d\omega} = -\tau. \tag{8}$$

As $d\varphi/d\omega$ is the group delay caused by the sample, simply by following the movement of the SPPs and determining their spectral positions at different time delays τ, the GD function of the sample can be obtained. Please note that usually just the relative time delay $\tau' = \tau + \varphi_1$, i.e. the sum of the time delay between the arms and the group delay introduced by the sample at the carrier frequency, is known, therefore only a relative group delay can be determined. By fitting a polynomial of appropriate order to the relative time delay curve, the dispersion coefficients describing the spectral phase can be determined

$$-\tau'_{fit} = x_0 + x_1\Delta\omega + x_2\Delta\omega^2 + x_3\Delta\omega^3 + x_4\Delta\omega^4, \tag{9}$$

where the fitting coefficients x_0, x_1, correspond to the coefficients of the Taylor-expansion of the spectral phase of the sample in Eq. (4), i.e. GD$=x_0+\varphi_1$, GDD$,=x_1$ TOD$=2x_2$, FOD$=6x_3$, QOD$=24x_4$ and $\Delta\omega = \omega - \omega_0$.

Introducing the group delay difference δGD(ω), a similar quantity to the spectral phase difference (see Eq. (2)) would be beneficial later:

$$\delta GD(\omega) = \frac{d\varPhi}{d\omega} = \varphi_1(\omega) + \tau, \tag{10}$$

where $\varphi_1(\omega)$ stands for the group delay function of the sample. Considering Eqs. (7) and (10) it becomes clear that the SPP is found at the frequency where the group delay difference is 0.

The importance of this method comes to light when high dispersion values are to be measured, as then the fringes at some parts of the interferogram might become too dense to be resolved by a spectrometer. Even so, in the vicinity of the SPPs the fringes become sparse enabling to locate their positions precisely. This problem arises in the case of any lower-order dispersion compensated stretcher-compressor system or fiber, where higher-order dispersion has greater significance or just in the case of long fibers.

3. Results and discussion

3.1. Simulations

Simulations were performed in order to demonstrate how specific dispersion coefficients affect the shape, movement and number of the SPPs. The case of dominant GDD is well-studied since the vast majority of optical elements represent such dispersion properties.

When the spectral phase is dominated by positive second-order dispersion, the value of the δGD equals to zero at only one frequency, thus one SPP forms, which travels toward higher frequencies as l_r is increased, i.e. τ decreased.

Grism pairs [7] or specialty fibers [23] can have dominant negative GDD, however, along a considerable amount of TOD. In this case the SPP moves toward the lower frequencies as the length of the reference arm is increased.

In most applications much effort is put toward reducing the second-order dispersion, thus avoiding the spreading of the input pulse. Since this can be achieved either by prism, grism or grating pairs or a specially designed fiber at the expense of an increment of the higher-order dispersion, hereinafter the effects on the shape, movement and number of the SPPs of different higher-order coefficients are discussed. First we investigated the effect of the TOD being the most significant term in the spectral phase by setting all other dispersion terms to zero

$$\delta GD(\omega) = \varphi_1 + \frac{\varphi_3}{2}\Delta\omega^2 + \tau = \frac{\varphi_3}{2}\Delta\omega^2 + \tau'. \tag{11}$$

The TOD was set to 100,000 fs^3 which is about the same order of magnitude as the characteristic of a grating pair with the gratings having 600-grooves/mm and placed 30 cm apart. A simulated normalized interferogram along with the group delay difference curves are shown in Fig. 1.

Due to the dominance of the TOD, the spectral phase was cubic, thus the δGD function was of second order. This means that at given lengths of the reference arm the value of the δGD became zero at two frequencies, therefore two SPPs formed on the interferogram. Note that this is not caused by polarization mode dispersion [28], nor by intermodal dispersion [32] but due to the prevalent presence of third-order chromatic dispersion as in Refs. [23,24]. Accordingly, in order to get the correct GD curve of the sample both SPPs should be monitored. The fact that the two SPPs symmetrically traveled away from each other as the length of the reference arms was increased (Fig. 2) confirmed that TOD was indeed positive, and the GDD was negligible.
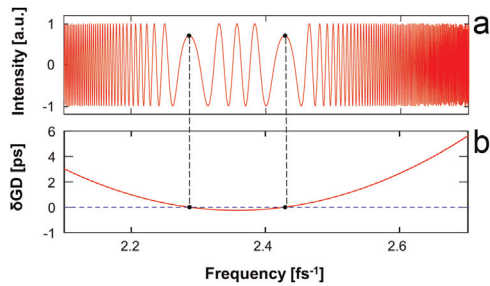
Fig. 1. (a) Simulated normalized interferogram for $TOD=+100,000$ fs^3 and $GDD=FOD=QOD=0$ belonging to 0 fs group delay difference at 2.285 and 2.427 fs^{-1}. (b) The corresponding group delay difference (red solid) curve. (For interpretation of the references to color in this figure legend, the reader is referred to the web version of this article.)
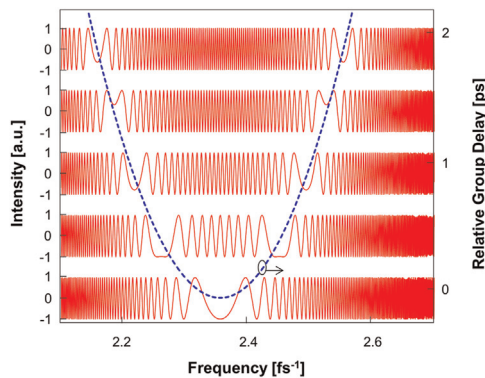

Fig. 2. Simulated normalized interferograms belonging to 50, -450, -950, -1450 and -1950 fs relative time delays τ', from the bottom to the top, respectively, and the relative group delay curve (blue dashed) calculated for $TOD=+100,000$ fs^3 and $GDD=FOD=QOD=0$ at 2.355 fs^{-1}. (For interpretation of the references to color in this figure legend, the reader is referred to the web version of this article.)

Note also that such dispersion values can cause thickening of the fringes at given time delays as it can be seen in the higher frequency regime in Fig. 2. In this case, due to the limited resolving power of the spectrometer, the visibility of the interferogram becomes lower aggravating its evaluation with most available methods. However, in the vicinity of the SPPs the fringes become sparse enabling to determine their spectral position accurately, thus evaluation based on the SPP method is feasible.

Since negative TOD can be generated by prism pairs or grism pairs [12] simulations were performed to investigate this case. By setting the TOD to $-10,0000$ fs^3 the GD curve switched from convex to concave and the SPPs travel toward each other as l_r was increased.

Next we analyzed the case of dominant FOD. Generally, optical elements, prism and grating pairs produce a negative FOD thus we also chose a negative value in our simulations. All the dispersion terms were set to zero and the FOD was chosen to be $-500,000$ fs^4, a value corresponding to the FOD of a grating pair with the gratings having 600-grooves/mm and placed 60 cm apart.

At the first glance this case is similar to the case of pure negative GDD, except that here the δGD curve is cubic, not linear. One SPP formed as for pure GDD, but as it can be seen from Fig. 3, it became too broad at some delays making the evaluation impossible in that frequency domain. Thickening of the interference fringes at some delays was also noticeable here, especially in the higher frequency regime.

Up to this point we can draw the conclusion that the SPP method is suitable for dispersion measurement when the GDD or the TOD is the dominant term in the spectral phase of the sample,
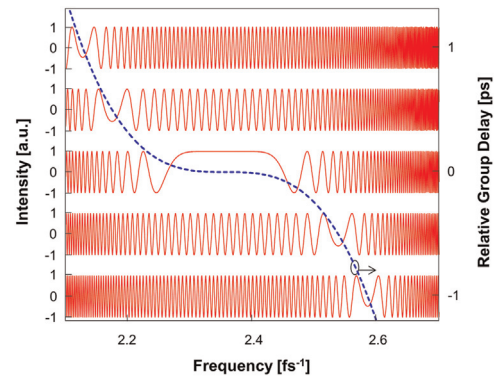

Fig. 3. Simulated normalized interferograms belonging to 1000, 500, 0, -500 and -1000 fs relative time delays τ', from the bottom to the top, respectively, and the relative group delay curve (blue dashed) calculated for $FOD=-50,0000$ fs^4 and $GDD=TOD=QOD=0$ at 2.355 fs^{-1}. (For interpretation of the references to color in this figure legend, the reader is referred to the web version of this article.)

however, it becomes inaccurate if FOD is prevalent. From the shape and number of the SPPs it is easy to tell which term is dominant.

In order to find out whether it is possible that more than two SPPs form on the interferogram additional simulations were performed. By setting different values for the dispersion terms, we found that the combination of the even phase terms resulted in three SPPs at some delays (see Fig. 4). The GDD was set to 3000 fs^2 and the FOD to $-500,000$ fs^4 while the other terms were zero. This can be the case when the TOD is completely compensated in a pulse stretcher or compressor still exhibiting residual GDD and FOD.

It can be seen that two or three SPPs can also appear. As the δGD was decreased by increasing l_r the SPP belonging to lower frequencies split in two and the newly formed one started to move towards the other SPP, belonging to higher frequencies, until they merged. Simultaneously the other newly formed SPP traveled in the opposite direction. In contrast to the case of the sole dominant FOD here the position of the SPPs could be precisely determined thus the SPP method is suitable for measuring such dispersion.

Similarly, we discovered that the combination of the odd dispersion coefficients can produce four SPPs at some delays (see Fig. 5). In the simulation the TOD of the sample was set to $-50,000$ fs^3 and the QOD to $+10^7$ fs^5. Although the QOD is not that significant in most cases, as recently revealed, photonic crystal and PBG fibers can exhibit QOD values of the same order of magnitude as used in the simulations [23,24].
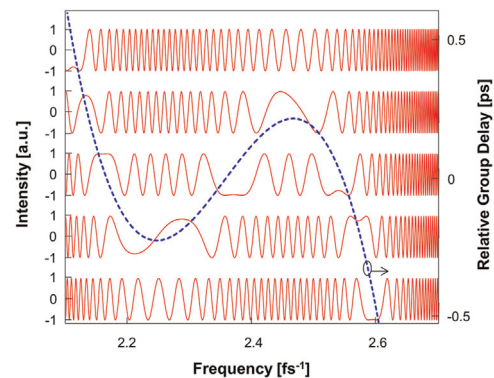

Fig. 4. Simulated normalized interferograms belonging to 400, 180, -40, -260 and -480 fs relative time delays τ', from the bottom to the top, respectively, and the relative group delay curve (blue dashed) calculated for $GDD=3,000$ fs^2, $FOD=-500,000$ fs^4 and $TOD=QOD=0$ at 2.355 fs^{-1}. (For interpretation of the references to color in this figure legend, the reader is referred to the web version of this article.)
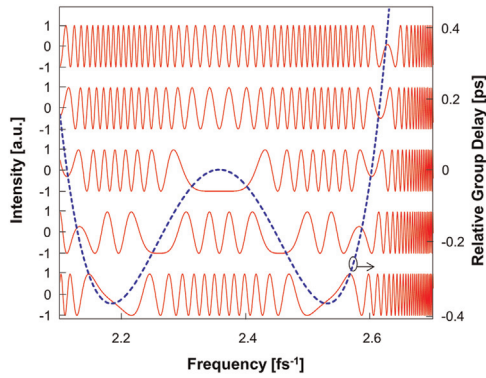
Fig. 5. Simulated normalized interferograms belonging to 400, 200, 0, −200 and −400 fs relative time delays τ', from the bottom to the top, respectively, and the relative group delay curve (blue dashed) calculated for TOD = −50,000 fs^3, QOD = +10^7 fs^5 and GDD = FOD = 0 at 2.355 fs^{-1}. (For interpretation of the references to color in this figure legend, the reader is referred to the web version of this article.)

Like in the previous cases, plotting interferograms belonging to different consecutive group delay differences together clearly outlines the shape of the GD curve (see Fig. 5). Note that at some delays two or three SPPs appeared. Even so, this case is distinguishable from the previous one, where the GDD and the FOD were dominant, as here the two SPPs both split in two as the delay was decreased, and the newly produced ones symmetrically traveled toward each other until they merged, creating a third one which shortly disappeared. In the case of combined dominant GDD and FOD this kind of symmetry was not present.

Summarizing the findings above it can be concluded that generally from the shape, movement and number of the SPPs it is possible to predict which dispersion terms are the most significant. In addition, the dispersion can be monitored, which is really beneficial when adjusting stretcher-compressor systems, for instance. However, in order to exclude any doubt regarding the dominance of given terms the dispersion coefficients should be also precisely determined by fitting a polynomial to the retrieved GD curve. With this method specialty fibers can be tested for higher-order dispersion in order to determine whether their quality is sufficient for the desired application.

3.2. Experimental results

Having the simulations performed the results were experimentally verified. First a 30.2 cm long Bragg-type solid-core PBG fiber having a quasi-periodic refractive index vs. radius profile with cylindrical symmetry was chosen as a sample, similar to the one used in Ref. [24]. The fiber was inserted in the sample arm of a Mach-Zehnder interferometer illuminated with a broadband Ti: Sapphire laser (FS rainbow, 6 fs at 800 nm, FWHM = 150 nm). The interference fringes were detected with a high resolution spectrometer (Ocean Optics HR4000, 700–900 nm, spectral resolution 0.1 nm). The CCD camera placed at the other output of the interferometer was used to facilitate the coupling. The experimental setup is illustrated in Fig. 6. The area denoted with dashed lines shows the adjustable part of the reference arm. A microscope objective (NA = 0.25, 10x) was used to couple the light into the fiber and a lens of 19 mm focal length was used to collimate the output pulses.

The coupling and the collimating lenses were placed in the reference arms, too, in order to compensate their dispersion. This way the interference pattern is only a result of the dispersion caused by the fiber. Fig. 7 shows recorded normalized interferograms. As established before if the fringes become too dense their visibility decreases due to the limited resolving power of the
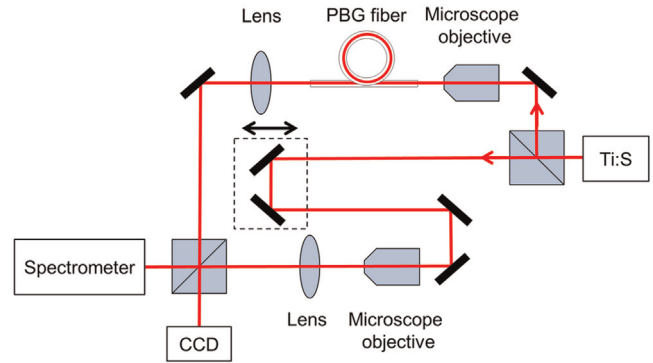

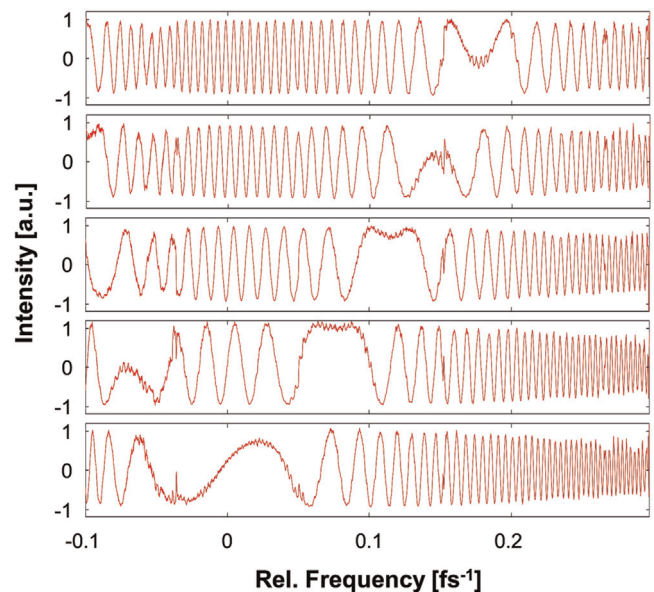**Fig. 6.** Spectrally resolved Mach–Zehnder interferometer with a PBG fiber.

Fig. 7. Recorded spectrally resolved and normalized interferograms of a PBG fiber belonging to −44, −311, −584, −846 and −1120 fs group delay differences at 2.355 fs^{-1}, from the bottom to the top, respectively.

spectrometer, the result of which is observable on some interferograms. As it can be seen at some delays two SPPs appeared on the interferograms which resembles the case of dominant positive TOD (see Fig. 2). Note that as shown in Ref. [24] this fiber has resonances at −0.038, 0.051 and 0.147 fs^{-1} which can be seen as sharp peaks on the interferograms. In the vicinity of these peaks the group delay difference becomes zero at two points, therefore, two SPPs are formed per peak. However, the poor wavelength resolution does not allow detecting these SPPs. The interferograms were evaluated with the SPP method and the retrieved GD curve is shown in Fig. 8. In order to dissolve any uncertainty the dispersion coefficient were also obtained up to the fifth order by fitting a fourth order polynomial to the curve (see Table 1).

By comparing these coefficients to the ones of a fused silica slab of the same length, calculated from [34], also shown in Table 1, it is evident that the PBG fiber has reduced GDD and increased TOD, both about two orders of magnitude. There is a considerable increase in the FOD and the QOD components of the PBG fiber also; however, they had no such effect on the SPPs as the TOD did, the dominance of which is confirmed also with the appearance of the two SPPs. The simulated GD curve (Fig. 1) also resembled the one retrieved with measurements (Fig. 8).

In the next measurements a fused silica prism pair with an apex angle of 67.5° served as a sample. In this case a
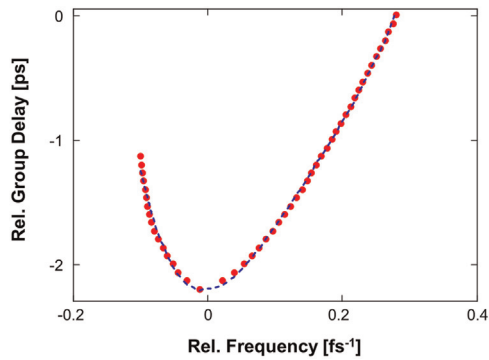
Fig. 8. Measured relative group delay of a PBG fiber as a function of the frequency (red dots) and the fitted fourth-order curve (blue dashed). (For interpretation of the references to color in this figure legend, the reader is referred to the web version of this article.)

Fig. 9. Spectrally resolved Michelson interferometer with a prism pair. WL: white-light source.

Michelson-interferometer was used which was illuminated with a tungsten halogen lamp (100 W) as illustrated in Fig. 9. Two lenses of 50 and 150 mm focal length were placed after the lamp in order to ensure the collimation of the beam. The prisms were placed 40 cm apart in the sample arm. By adjusting the end mirror in the reference arm different delays were set. Using a flip mirror, a lens of 300 mm focal length and a polarity rotator (periscope) the beam was directed into a spectrograph (CE Optics, CEO-2D-800-V, 700–900 nm, spectral resolution 0.15 nm) to verify that no residual angular dispersion was present thus the prism pair was well-set. Otherwise the interferograms were observed with a lower resolution spectrometer (Avantes 3648, 200–1100 nm, spectral resolution 1 nm) in order to widen the detection range.

Measurements were performed by adjusting the optical path length in the second prism in order to generate different dispersion properties and to test whether the SPPs suggest the presence of different orders. In the first measurements the optical path length in the prisms was reduced to its minimum which resulted in the appearance of one SPP which moved toward the lower frequencies as the delay between the two arms was decreased (Fig. 10(a)) indicating negative GDD. As the path in glass was increased two SPPs appeared at some delays (Fig. 10(b)) suggesting the dominance of the TOD. Introducing more glass to the system produced one SPP again, however, in this case it was moving toward the higher frequencies (Fig. 10(c)) with decreasing delay which marks positive GDD. Despite that as a result the visibility of the fringes radically decreased at some delays the positions of the SPPs could be determined in all cases.

After evaluating the recorded interferograms with the SPP method we retrieved the GD curves. Note that only the GD curve belonging to Fig. 10(b) is shown in Fig. 11 as the other two cases are trivial. By fitting a third-order polynomial to the curves the dispersion coefficients were calculated up to the fourth order (Table 1). In the case of the least and the most glass in the system the GDD is negative and positive, respectively, as it was predicted. For the case of the two SPPs, as it can be seen, the value of the TOD is small in contrast to our prediction. However, the joint effect of
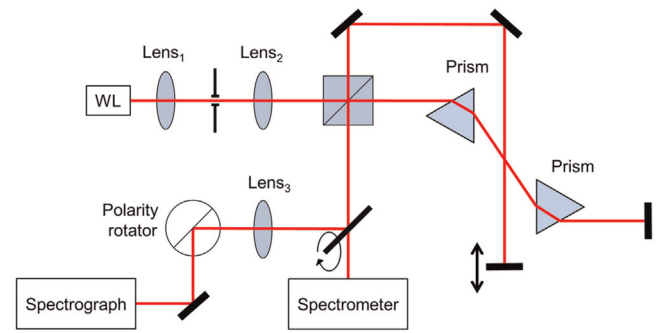
the GDD and the FOD can also produce two SPPs as seen in the simulations (see Fig. 4). Note that here the relatively small dispersion coefficients caused the resemblance to the case of dominant TOD because the scanned spectral interval was smaller than it should be in order to demonstrate the full path of the SPPs. Even so, during adjustment of prism pairs in most cases it is enough to reveal whether higher-order dispersion is present which is demonstrated by the presence of more than one SPP. For pulse stretcher-compressor systems this problem does not arises because the large values of the dispersion coefficients. Considering that the retrieval of the dispersion coefficients up to the fifth order proved to be unnecessary and resulted in false values, it is safe to conclude that the QOD is insignificantly small, thus this case cannot be mistaken for the case of joint dominant TOD and QOD.

4. Summary

A detailed study regarding the applicability of the SPP method in monitoring of the dominance of the higher-order dispersion was performed. The effects on the shape, movement and number of the SPPs of different dispersion terms up to the fifth order were studied using simulations. It was shown that in contrast to the well-known case of a glass slab with dominant GDD different dispersion terms or their combinations could result in the appearance of more than one SPP. Dominant TOD produced two, joint GDD and FOD three and joint TOD and QOD four SPPs. The positions of the SPPs could be precisely determined in all cases except for sole dominant FOD where it became too broad. Based on the results of the simulations it can be concluded that by analyzing the shape, movement and number of the SPPs it can be anticipated which dispersion term has the most significance, yet retrieval of the coefficients facilitates excluding any uncertainties regarding the dominant terms.

Having the simulations performed the results were compared with measurements conducted on a PBG fiber and a prism pair. Based on the comparison to a fused silica slab of the same length we concluded that the GDD of the PBG fiber was reduced, which resulted in the increment of the TOD, FOD and QOD component. Although the FOD and the QOD in the case of the PBG fiber were

Table 1

Dispersion coefficients of the 30.2 cm long PBG fiber, of a conventional fused silica slab of the same length and of the fused silica prism pair with an apex angle of 67.5° placed 40 cm apart with the shortest[a], the second shortest[b] and longest paths[c] in the second prism.

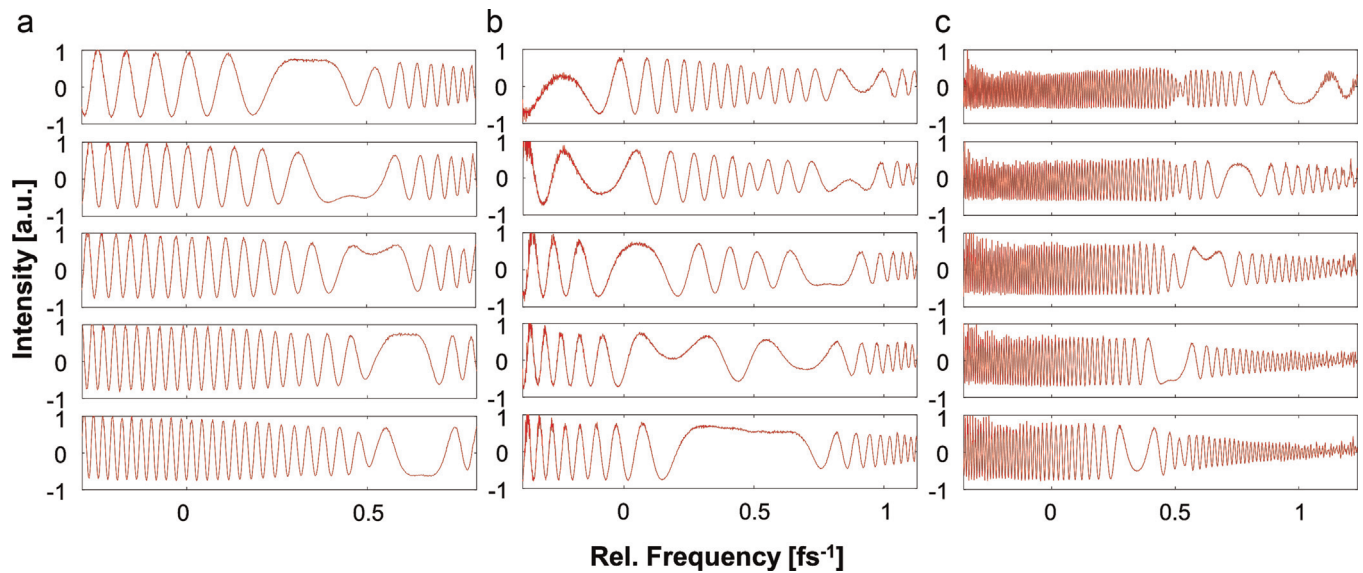|	GDD [fs^2]	TOD [fs^3]	FOD [fs^4]	QOD [fs^5]
PBG fiber	697 ± 36	$1.391 \times 10^5 \pm 360$	$-1.75 \times 10^6 \pm 2.11 \times 10^4$	$1.17 \times 10^7 \pm 2.25 \times 10^5$
Fused silica slab	1.09×10^4	8.3×10^3	-3.45×10^3	9.59×10^3
Prism pair[a]	-100 ± 2	-155 ± 67	$-2.195 \times 10^3 \pm 192$	/
Prism pair[b]	245 ± 9	-80 ± 26	$-1.918 \times 10^3 \pm 23$	/
Prism pair[c]	950 ± 6	342 ± 45	$-1.323 \times 10^3 \pm 105$	/

Fig. 10. Recorded spectrally resolved and normalized interferograms of a prism pair at different prism positions belonging to (a) 221, 188, 141, 105 and 64 fs, (b) 53, 22, −12, −41 and −68 fs, (c) −334, −462, −593, −709 and −838 fs group delay differences at 2.355 fs^{-1}, from the bottom to the top, respectively.
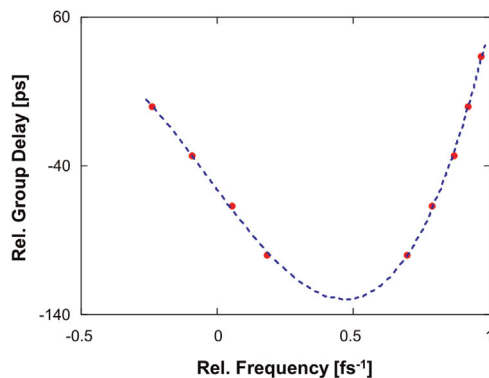

Fig. 11. Measured relative group delay of a prism pair as a function of the frequency (red dots) and the fitted third-order curve (blue dashed). (For interpretation of the references to color in this figure legend, the reader is referred to the web version of this article.).

also higher than that of the silica slab they had no such effect on the SPPs as the TOD did. The dominance of the TOD was also confirmed by comparing the recorded interferograms to the simulated ones, as in the case of the PBG fiber two SPPs were present like in the simulations, where the TOD was set dominant. The simulated GD curve also resembled the one retrieved with measurements. In the case of the prism pair the co-dominance of the GDD and the FOD was revealed as despite the small value of the TOD and the insignificance of the QOD two SPPs appeared at some delays. This fact suggests that in the case of small dispersion values either retrieving of the dispersion coefficients or increasing the scanned spectral interval is beneficial to rule out any ambiguity that might be present.

The findings of the work are useful when higher-order dispersion is measured, which is an often feature of specially designed photonic crystal and PBG fibers, in assistance to their further development or quality testing. Yet another aspect is that studying the shape, movement and number of the SPPs allows a quasi-real-time monitoring possibility of the residual higher-order dispersion which can be quite advantageous when adjusting stretcher-compressor systems, especially when combined with a LabVIEW control unit.

References

[1] P. Yeh, A. Yariv, E. Marom, Theory of Bragg fiber, J. Opt. Soc. Am. 68 (1978) 1196–1201.
[2] J.C. Knight, T.A. Birks, P. St., J. Russell, D.M. Atkin, All-silica single-mode optical fiber with photonic crystal cladding, Opt. Lett. 21 (1996) 1547–1549.
[3] J. Broeng, D. Mogilevstev, S.E. Barkou, A. Bjarklev, Photonic crystal fibers: a new class of optical waveguides, Opt. Fiber Technol. 5 (1999) 305–330.
[4] St.P.J. Russell, Photonic-crystal fibers, J. Lightwave Technol. 24 (2006) 4729–4749.
[5] Z. Várallyay, K. Saitoh, J. Fekete, K. Kakihara, M. Koshiba, R. Szipőcs, Reversed dispersion slope photonic bandgap fibers for broadband dispersion control in femtosecond fiber lasers, Opt. Express 16 (2008) 15603–15615.
[6] D. Strickland, G. Mourou, Compression of amplified chirped optical pulses, Opt. Commun. 56 (1985) 219–221.
[7] P. Tournois, New diffraction grating pair with very linear dispersion for laser pulse compression, Electron. Lett. 29 (1993) 1414–1415.
[8] W.E. White, F.G. Patterson, R.L. Combs, D.F. Price, R.L. Shepherd, Compensation of higher-order frequency-dependent phase terms in chirped-pulse amplification systems, Opt. Lett. 18 (1993) 1343–1345.
[9] B.E. Lemoff, C.P.J. Barty, Quintic-phase-limited, spatially uniform expansion and recompression of ultrashort optical pulses, Opt. Lett. 18 (1993) 1651–1653.
[10] P. Tournois, Nonuniform optical diffraction gratings for laser pulse compression, Opt. Commun. 106 (1994) 253–257.
[11] C. Fiorini, C. Sauteret, C. Rouyer, N. Blanchot, S. Seznec, A. Migus, Temporal aberrations due to misalignments of a stretcher-compressor system and compensation, IEEE J. Quantum Electron. 30 (1994) 1662–1670.
[12] S. Kane, J. Squier, Grism-pair stretcher-compressor system for simultaneous second- and third-order dispersion compensation in chirped-pulse amplification, J. Opt. Soc. Am. B 14 (1997) 661–665.
[13] S. Kane, J. Squier, Fourth-order-dispersion limitations of aberration-free chirp-pulse amplification system, J. Opt. Soc. Am. B 14 (1997) 1237–1244.
[14] E.A. Gibson, D.M. Gaudiosi, H.C. Kapteyn, R. Jimenez, S. Kane, R. Huff, C. Durfee, J. Squier, Efficient reflection grisms for pulse compression and dispersion compensation of femtosecond pulses, Opt. Lett. 31 (2006) 3363–3365.

[15] J.C.M. Diels, J.J. Fontaine, I.C. McMichael, F. Simoni, Control and measurement of ultrashort pulse shapes (in amplitude and phase) with femtosecond accuracy, Appl. Opt. 24 (1985) 1270–1282.

[16] R. Trebino, K.W. DeLong, D.N. Fittinghoff, J.N. Sweetser, M.A. Krumbügel, B. A. Richman, D.J. Kane, Measuring ultrashort laser pulses in the time-frequency domain using frequency-resolved optical gating, Rev. Sci. Instrum 68 (1997) 3277–3295.

[17] T. Hirayama, M. Sheik-Bahae, Real-time chirp diagnostic for ultrashort laser pulses, Opt. Lett. 27 (2002) 860–862.

[18] A.K. Sharma, P.A. Naik, P.D. Gupta, Estimation of higher order chirp in ultrashort laser pulses using modified spectrum auto-interferometric correlation, Opt. Commun. 233 (2004) 431–437.

[19] B. Yellampalle, R.D. Averitt, A.J. Taylor, Unambiguous chirp characterization using modified-spectrum auto-inerferometric correlation and pulse spectrum, Opt. Express 14 (2006) 8890–8899.

[20] D.A. Bender, J.W. Nicholson, M. Sheik-Bahae, Ultrashort laser pulse characterization using modified spectrum auto-interferometric correlation (MOSAIC), Opt. Express 16 (2008) 11782–11794.

[21] T.M. Shuman, M.E. Anderson, J. Bromage, Ch. Iaconis, L. Waxer, I.A. Walmsley, Real-time SPIDER: ultrashort pulse characterization at 20 Hz, Opt. Express 5 (1999) 134–143.

[22] G. Stibenz, C. Ropers, Ch. Lienau, Ch. Warmuth, A.S. Wyatt, I.A. Walmsley, G. Steinmeyer, Advanced methods for the characterization of few-cycle light pulses: a comparison, Appl. Phys. B 83 (2006) 511–519.

[23] T. Grósz, R. Szipöcs, and A.P. Kovács, Measurement of polarization-dependent chromatic dispersion in a birefringent hollow-core photonic crystal fiber using spectral interferometry, in Workshop on Specialty Optical Fibers and their Applications, (Optical Society of America, 2013), paper F2.10.

[24] T. Grósz, A.P. Kovács, M. Kiss, R. Szipőcs, Measurement of higher order chromatic dispersion in a photonic bandgap fiber: comparative study of spectral interferometric methods, Appl. Optics 53 (2014) 1929–1937.

[25] C. Sáinz, P. Jourdain, R. Escalona, J. Calatroni, Real time interferometric measurements of dispersion curves, Opt. Commun. 111 (1994) 632–641.

[26] R. Szipöcs, A.P. Kovács, Dispersion measurement on crystals for ultrashort pulse generation with use of interference in the frequency domain, in Conference on Lasers and Electro-Optics 11 OSA Technical Digest Series (Optical Society of America, Washington D.C., 1997), paper CTuP32.

[27] L.M. Simohamed, F. Reynaud, Characterisation of the dispersion evolution versus stretching in a large stroke optical fibre delay line, Opt. Commun. 159 (1999) 118–128.

[28] P. Hlubina, D. Ciprian, L. Knyblová, Direct measurement of dispersion of the group refractive indices of quartz crystal by white-light spectral interferometry, Opt. Commun. 269 (2007) 8–13.

[29] P. Hlubina, J. Olszewski, Phase retrieval from spectral interferograms including the stationary-phase point, Opt. Commun. 285 (2012) 4733–4738.

[30] H.-T. Shang, Chromatic dispersion measurement by white-light interferometry on metre-length single-mode optical fibres, Electron. Lett. 17 (1981) 603–605.

[31] F. Koch, S.V. Chernikov, J.R. Taylor, Dispersion measurement in optical fibres over the entire spectral range from 1.1 μm to 1.7 μm, Opt. Commun. 175 (2000) 209–213.

[32] P. Hlubina, White-light spectral interferometry to measure intermodal dispersion in two-mode ellipitical-core optical fibres, Opt. Commun. 218 (2003) 283–289.

[33] A.P. Kovács, K. Osvay, G. Kurdi, M. Görbe, J. Klebniczki, Z.s. Bor, Dispersion control of a pulse stretcher-compressor system with two dimensional spectral interferometry, Appl. Phys. B 80 (2005) 165–170.

[34] I.H. Malitson, Interspecimen comparison of the refractive index of fused silica, J. Opt. Soc. Am. 55 (1965) 1205–1208.